
VEHICLE TRAJECTORY PREDICTION IN CITY-SCALE ROAD NETWORKS USING A DIRECTION-BASED SEQUENCE-TO-SEQUENCE MODEL WITH SPATIOTEMPORAL ATTENTION MECHANISMS

Yuebing Liang

Department of Urban Planning and Design
University of Hong Kong
Hong Kong
u3007104@connect.hku.hk

Zhan Zhao*

Department of Urban Planning and Design
University of Hong Kong
Hong Kong
zhanzhao@hku.hk

ABSTRACT

Trajectory prediction of vehicles at the city scale is of great importance to various location-based applications such as vehicle navigation, traffic management, and location-based recommendations. Existing methods typically represent a trajectory as a sequence of grid cells, road segments or intention sets. None of them is ideal, as the cell-based representation ignores the road network structures and the other two are less efficient in analyzing city-scale road networks. In addition, most models focus on predicting the immediate next position, and are difficult to generalize for longer sequences. To address these problems, we propose a novel sequence-to-sequence model named D-LSTM (Direction-based Long Short-Term Memory), which represents each trajectory as a sequence of intersections and associated movement directions, and then feeds them into a LSTM encoder-decoder network for future trajectory generation. Furthermore, we introduce a spatial attention mechanism to capture dynamic spatial dependencies in road networks, and a temporal attention mechanism with a sliding context window to capture both short- and long-term temporal dependencies in trajectory data. Extensive experiments based on two real-world large-scale taxi trajectory datasets show that D-LSTM outperforms the existing state-of-the-art methods for vehicle trajectory prediction, validating the effectiveness of the proposed trajectory representation method and spatiotemporal attention mechanisms.

Keywords Trajectory prediction · Trajectory representation · Road networks · Sequence-to-sequence modeling · Spatiotemporal attention

1 Introduction

With the widespread use of mobile sensors, such as GPS devices and smartphones, it is possible to track all kinds of moving objects in a near real-time fashion. The increasing prevalence of localization technologies has resulted in large volumes of trajectory data which record the spatiotemporal footprints of vehicles. These data often contain valuable information, which gives rise to many location-based services and applications such as vehicle navigation [1], traffic management [2] and location-based recommendations [3]. Many of these applications rely on the ability to dynamically predict vehicle routing behavior. For example, if the path of vehicles is known in advance, intelligent transportation systems can provide personalized assistance or recommendation functions to drivers, such as dynamic rerouting, personalized risk assessment and mitigation, speed advice and engine management systems. In addition, trajectory prediction is essential for traffic managers to anticipate possible upcoming hazards, future congestion and travel delays, and deploy traffic control and management strategies accordingly. Based on trajectory prediction, it's also

*Corresponding Author

possible to develop customized location-based advertising for those most likely to pass through certain business outlets and shops [4].

Extensive researches have been done to address the problem of vehicle trajectory prediction in previous works. Traditional approaches mostly depend on probabilistic graphical models for vehicle trajectory prediction [4, 5, 6], which usually rely on one or two previous locations to predict the next one based on variants of Markov models. Recently, with the rapid advance in deep learning, a number of deep neural network models have been developed to address vehicle behavior prediction problems [7, 8, 9]. Many related approaches are developed for autonomous driving applications [10]. They usually focus on a specific road section and predict the states of the nearby vehicles in the next few seconds. These models are not applicable to the city-scale vehicle trajectory prediction problem due to the drastically different time and spatial scales. Only a few recent studies attempted to predict the route choice of a vehicle approaching an intersection by pre-defining an intention set of going straight, turning left, turning right and so on [11, 12]. Despite extensive researches, there still exist a few research gaps to be addressed:

- Existing methods represent vehicle trajectories as sequences of grid cells, road segments or intention sets, none of which are ideal. First, grid-cell based representation fails to consider the topological structure of the road network, and is not suitable for applications based on the road network (e.g., dynamic routing). Second, the use of road segments may lead to data sparsity and high dimensionality issues, especially when the road network is large and complex. Third, for the intention-based trajectory representation, it is hard to predetermine all possible driving intentions in a big and complex driving network [10].
- Existing approaches mostly focus on the next position prediction and are difficult to generalize for long-term sequential patterns. One main reason is that it is computationally costly for sequence prediction since the number of candidate sequences is exponential to the length of the sequence [13]. As a result, existing trajectory prediction algorithms tend to have relatively low prediction accuracies for long-range trajectory prediction.

Therefore, despite existing studies, vehicle trajectory prediction in city-scale road networks is still a challenging problem and requires innovative solutions. To solve this problem, this paper proposes a novel direction-based sequence-to-sequence (seq2seq) model with spatiotemporal attention mechanisms, named D-LSTM (or Direction-based Long Short-Term Memory), for vehicle trajectory prediction in city-scale road networks. In the proposed model, a direction-based trajectory representation method is performed so that both the input and output sequences of road segments are replaced with sequences of intersections and associated movement directions. Subsequently, an embedding layer transforms the intersection and direction information into a latent space and a spatial attention layer is used to capture spatial dependencies in the road network. The embedded information is then fed to a LSTM encoder-decoder module with a sliding temporal attention mechanism to capture temporal interaction across the input and output trajectories. Finally, an output layer is used to generate future trajectories. The model is evaluated based on two real-world datasets of taxi GPS trajectories from Shanghai and Beijing. The main contributions of this paper are as follows:

- We propose a seq2seq model for vehicle trajectory prediction in a city-scale road network. To the best of our knowledge, our proposed model is the first deep learning-based trajectory prediction model that accounts for the structure of road networks at such large scale.
- We introduce a direction-based trajectory representation approach which represents each road segment as a pair of intersection and associated movement direction. This helps reduce the prediction dimensionality from over 100,000 road segments to a small number of direction labels (8 in our experiment settings), which improves both the modeling efficiency and prediction accuracy.
- We develop a novel LSTM encoder-decoder architecture with spatial and temporal attention mechanisms that can dynamically model spatiotemporal dependencies in complex road networks.
- Comprehensive experiments are conducted based on real-world taxi trajectory data from Shanghai and Beijing. The results show that our model outperforms state-of-the-art methods, and all the new model components improve the prediction performance.

This paper is structured as follows. Section 2 discusses related work and limitations. The problem statement and our proposed D-LSTM model is introduced in Section 3, and our numerical experiments, including datasets and results are presented in Section 4. The paper is concluded in Section 5.

2 Related Work

As prior studies adopted different representations of trajectories, we will first review the methods for trajectory representation, before discussing specific models for trajectory prediction.

2.1 Trajectory Representation

Trajectory representation is a mathematical abstraction of trajectory data necessary for modeling. Depending on how a vehicle’s location is represented, there are three major trajectory representation methods: cell-based, link-based, and intention-based.

In cell-based representation, the geographic area is divided into regular-shaped cells, and the vehicle’s location is aggregated to the corresponding cell. Zhou et al. [14] presented a “semi-lazy” approach for trajectory prediction which divides the study area into a set of uniform cells and the model outputs the predicted grid cell that the vehicle will visit next. Pecher et al. [15] proposed a vehicle trajectory prediction model based on Markov models and artificial neural networks by dividing the study area to a grid of cells, each a 1.25km-by-1.25km area. A k-d tree-based space discretization is performed in [16], aggregating GPS locations to discrete cells, each of which contains a defined number of data points. Lv et al. [17] mapped trajectories to two-dimensional grid images and applied a convolutional neural network model for trajectory destination prediction. While a cell-based representation is useful for certain applications (e.g., destination prediction), this method has several limitations for trajectory prediction: (1) it does not consider the topological structure of the actual road network; and (2) aggregation by land cells is typically too coarse for certain applications (e.g., routing) that require the precise vehicle path along the road network.

Link-based representation maps the vehicles’ GPS locations to road network segments using map matching techniques [18]. The trajectory is expressed as a series of road segments, and the problem of trajectory prediction is to determine the next series of road segments the vehicle will visit. Liu and Karimi [19] introduced a probability-based model that estimates the probability of taking each road segment at each intersection. In [1], the road network is represented with trajectory-level characteristics and taxi trajectories are predicted given known destinations based on probabilistic reasoning from observed context-aware behavior. Tang et al. [20] adopted a Hidden Markov Model (HMM) to predict the next route choice of taxis and employed a linear motion function to estimate the taxi’s future location. The main drawback of link-based representation is the large number of road segments in big cities, which not only increases the data sparsity problem [21], but also poses challenges to statistical modeling.

Intention-based representation describes vehicle behavior with an intention set such as going straight, turning left, turning right and so on. Philips et al. [22] applied an LSTM model to predict whether a driver will turn left, turn right or go straight at an intersection. Zyner et al. [11] defined an intention set of going east, west or south based on vehicle destination to predict the routing behavior of a vehicle approaching a T-junction. Ding et al. [12] extended the intention-based representation to highway driving scenarios, and predicted lane change and lane keeping behavior of vehicles. One main drawback of these approaches is that it is difficult to predetermine all possible driving intentions in large-scale complex road networks [10].

2.2 Trajectory Prediction

Existing trajectory prediction methods can be grouped into two categories: probabilistic graphical models and deep learning models. Probabilistic graphical models, especially variants of Markov-chain (MC) models, have been widely used to mine frequent patterns for mobility prediction problems. Asahara et al. [23] proposed a mixed MC model that considers both individual and generic effects for pedestrian movement prediction. An extended MC model was adopted to predict the next location of an individual based on previous n locations [24]. More generally, a Bayesian n -gram model was introduced to mine spatiotemporal dependencies for next trip prediction [25]. Rathore et al. [4] proposed a scalable clustering and MC-based trajectory prediction framework which can handle large volumes of trajectory data. In addition, HMM is also often used to model mobility sequences or vehicle trajectories [5, 6, 26]. There are three main drawbacks in these methods: (1) they rely on one or two previous locations for trajectory prediction while fail to consider long-term temporal dependencies; (2) they mostly focus on the next location prediction while perform poorly for long-range trajectory prediction; and (3) they are not as flexible for capturing the environment and other external factors.

Deep learning models for trajectory prediction usually treat it as a seq2seq problem, which takes one sequence as input and outputs another. Seq2seq models are widely used in natural language processing [27, 28]. Most seq2seq models employ Recurrent Neural Networks (RNN) and a series of its derivatives, such as Bidirectional Recurrent Neural Network (BiRNN) [29], Long Short-Term Memory (LSTM) [30] and Gated Recurrent Unit (GRU) [31]. Several studies have adopted various RNN methods for trajectory prediction. Park et al. [7] proposed a seq2seq prediction technique of vehicle trajectories using LSTM encoder-decoder architecture. Wang et al. [9] proposed a multi-vehicle collaborative learning for vehicle trajectory prediction which leverages LSTM encoder-decoder model for trajectory generation. More recently, attention-based recurrent architecture [27] was proposed to capture long-term temporal dependencies by adaptively paying more attention to relevant hidden states. Inspired by this, Li et al. [32] developed a hierarchical temporal attention-based LSTM encoder-decoder model for long-term human location sequence prediction.

Li et al. [33] devised a Simple Recurrent Units (SRU)-based trajectory prediction model and developed an attention mechanism to enhance SRU. To reduce sequential computation of RNNs, Transformer was proposed in [28], which relies entirely on self-attention network dispensing with RNNs. In this study, we apply an attention-based LSTM in our model and compare the performance of different seq2seq models for trajectory prediction. Despite progress in deep learning for trajectory prediction, existing approaches are usually implemented in a small study area with cell-based trajectory representation. Moreover, existing deep learning methods are not suitable for large-scale road networks, as the large number of output neurons can limit the model efficiency and prediction performance.

3 Methodology

In this section, we first introduce our problem statement and then propose a new framework for trajectory prediction in city-scale road networks. As shown in Fig. 1, the proposed framework comprises of five modules: (1) a trajectory representation module that transforms the input and output trajectories into an intersection sequence and a direction sequence, (2) an embedding layer that encodes the intersection and direction information, (3) a spatial attention layer that captures the spatial dependencies in urban road networks, (4) a LSTM encoder-decoder module with temporal attention mechanism that captures temporal dependencies in trajectories, and (5) an output layer that incorporates other context features and outputs the predicted trajectory.

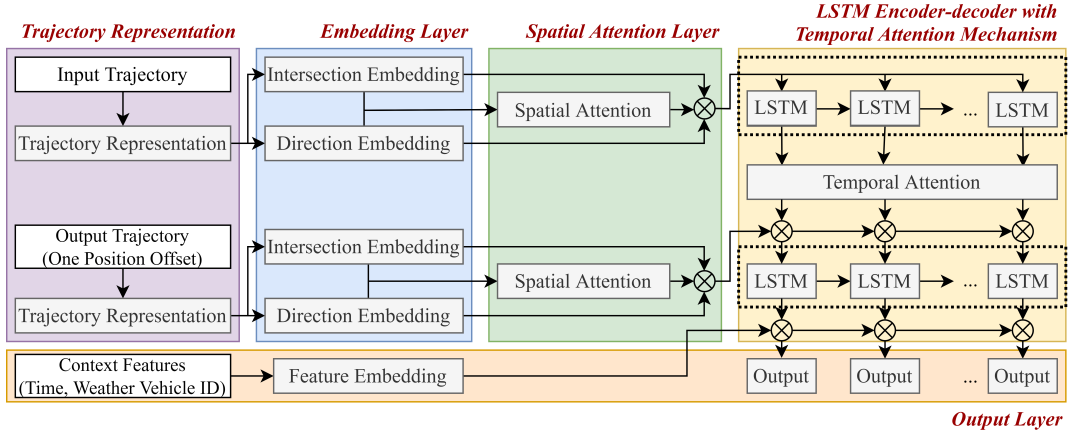


Figure 1: Architecture of the proposed trajectory prediction model (\otimes represents the concatenation operation)

3.1 Definitions and Problem Statement

Definition 1 (Road Network): The road network is represented as a directed graph $G = (N, E)$, which is composed of a set of intersection nodes N and a set of road segments E . Each road segment $e \in E$ can be represented as $e = (e.\text{source}, e.\text{target})$, where $e.\text{source}, e.\text{target} \in N$ are the source and target nodes of road segment e respectively.

Definition 2 (Trajectory): a trajectory T of length l comprises l connected road segments in time series, and is expressed as $T = \{e_1, e_2, \dots, e_l\}$ where $e_i \in E, 1 \leq i \leq l, e_i.\text{target} = e_{i+1}.\text{source}$.

Problem: given a prefix trajectory of length l_{in} denoted as $X = \{e_{1-l_{in}}, \dots, e_{-1}, e_0\}$ where a vehicle orderly visited, the trajectory prediction problem aims to predict the future trajectory of length l_{out} denoted as $Y = \{e_1, e_2, \dots, e_{l_{out}}\}$ that the vehicle will traverse.

3.2 Trajectory Representation

In order to preserve the road network typology while overcoming the problem of high prediction dimensionality, a direction-based trajectory representation approach is proposed. The general idea of the approach is to map each road segment to a unique label as $e = (e.\text{source}, e.\text{direction})$, where $e.\text{direction}$ is a categorical feature indicating the rough direction of e . As we will demonstrate later, this new representation can greatly simplify the trajectory prediction problem. The direction-based trajectory representation is composed of 3 steps.

Step 1: Calculate the specific heading direction of each road segment. Given e , we use $e.heading$ to denote the heading direction from $e.source$ to $e.target$. The basis of heading direction is north.

Step 2: Discretize $e.heading$ based on predefined intervals. Specifically, the heading range $[0, 360)$ is partitioned into K equal intervals, each having the same width $W = 360/K$. Each road segment e is mapped to the interval $e.interval$ using:

$$e.interval = \lfloor \frac{e.heading}{W} \rfloor \quad (1)$$

Fig. 2a illustrates Steps 1 and 2, assuming $K = 8$. In this example, $e_1.heading = 50$ degrees, and $e_1.interval = II$ (the second interval).

Step 3: Map each road segment $e = (e.source, e.target)$ to a new representation $e = (e.source, e.direction)$. Initially, $e.direction = e.interval$. However, there may be more than one road segments with the same $e.interval$ in some occasions. If road segment e' shares the same representation with another road segment e , where $e.source = e'.source$ and $e.interval = e'.interval$, we would redefine $e'.direction$ to the closest *available* interval to $e'.heading$. An interval is available if there is no other road segment starting from the same source with the same interval. Fig. 2b shows an example. Note that while such revision might influence the accuracy of the direction representation of some roads, the influence is trivial since only a small portion of roads require revisions. It is uncommon to see more than one road segments that start from the same intersection and are less than 45 degrees apart. For example, in the road network of Shanghai, when $K = 8$ only 2% road segments require revision to their direction labels.

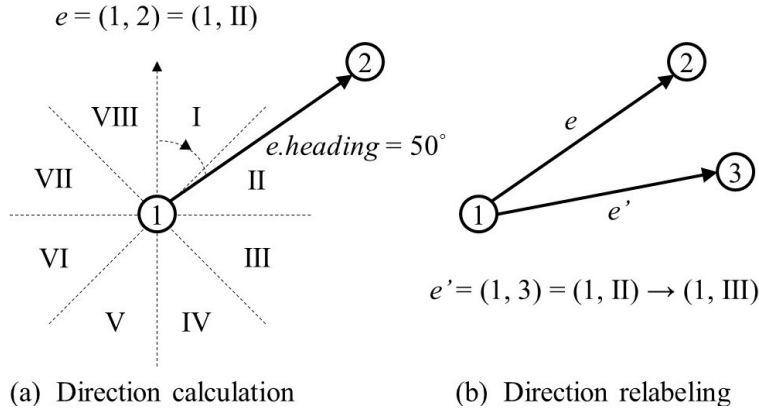


Figure 2: Direction-based trajectory representation approach

Using our proposed direction-based trajectory representation method, each road segment e is mapped to a unique combination $(e.source, e.direction)$. This means that given the source node and direction, we can uniquely identify the target node. For the i -th road segment in a trajectory e_i , we denote $n_{i-1} = e_i.source$, $n_i = e_i.target$, and $r_i = e_i.direction$. An example of the new trajectory after trajectory representation is shown in Fig. 3. Based on this new representation, we can predict a future trajectory $Y = \{e_1, e_2, \dots, e_{l_{out}}\}$ by simply predicting its associated direction sequence $Y_R = \{r_1, r_2, \dots, r_{l_{out}}\}$ (assuming n_0 is given). Algorithm 1 shows how we may use Y_R to reconstruct the corresponding node sequence $Y_N = \{n_1, n_2, \dots, n_{l_{out}}\}$ as well as Y . Note that Y_R has much lower dimensionality than Y , and should be more predictable, which is the main advantage of the proposed trajectory presentation method. For the input trajectory $X = \{e_{1-l_{in}}, \dots, e_{-1}, e_0\}$, we would preserve as much information as possible by using both the direction sequence $X_R = \{r_{1-l_{in}}, \dots, r_{-1}, r_0\}$, and node sequence $X_N = \{n_{1-l_{in}}, \dots, n_{-1}, n_0\}$.

3.3 Embedding Layer

The node and direction sequences cannot be fed into neural networks directly. The embedding layer maps them to a low-dimensional latent space. Specifically, an intersection embedding layer first maps each intersection node $n \in N$ to a latent vector $v_n \in \mathbb{R}^M$ by learning a parameter matrix $W_n \in \mathbb{R}^{M \times |N|}$. Similarly, the direction embedding layer maps each direction r to a vector $v_r \in \mathbb{R}^D$ by multiplying a parameter matrix $W_r \in \mathbb{R}^{D \times K}$ to its one-hot representation. M and D are the latent vector dimensions for node n and direction r respectively. Parameters of W_n, W_r are learned simultaneously with all other parameters through model training.

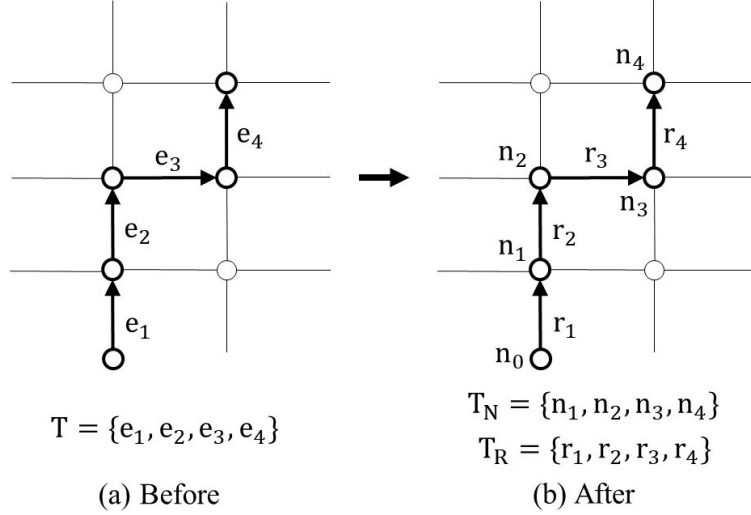


Figure 3: Trajectory before and after direction-based trajectory representation

Algorithm 1: Generating output trajectory Y from output direction sequence Y_R

Input : output direction sequence $Y_R = \{r_1, r_2, \dots, r_{l_{out}}\}$, the last intersection of input intersection sequence n_0

Output: output trajectory $Y = \{e_1, e_2, \dots, e_{l_{out}}\}$

$$Y = \{\};$$

for i in $\{1, 2, \dots l_{out}\}$ **do**

Find the next node n_i according to the unique label (n_{i-1}, r_i) ;

$$e_i = (n_{i-1}, n_i);$$

1

end

3.4 Spatial Attention Layer

While the embedding layer captures spatial information of each intersection through observed vehicle trajectories, it does not explicitly consider the road network typology. Inspired by Graph Attention Networks [34], we develop a spatial attention mechanism to model the spatial dependencies of intersections in the urban road network. Specifically, the road network is treated as a graph, where each intersection corresponds to a node and each road segment to an edge. In the spatial attention layer, adjacent nodes pass messages to each other and an attention mechanism is applied to calculate the weighted influence (i.e., attention weights) between adjacent nodes. For each intersection node in trajectories, the spatial attention layer generates a context vector as a weighted sum of the features of its adjacent intersections. Fig. 4 illustrates the message passing mechanism in the spatial attention layer.

For each intersection n in trajectories, a spatial context vector $w_n \in \mathbb{R}^M$ is built with the following four steps:

Step 1: Identify adjacent intersection nodes for an intersection n , denoted as $n.neighbor$. We impose a spatial context window where nodes only pass messages to adjacent nodes that connect with node n directly. The spatial context window allows the spatial attention layer to make use of the connectivity structure of the road network and implement message passing more efficiently.

Step 2: Compute the importance score of each adjacent node n' to node n given as:

$$s_{nn'} = [v_n; v_{n'}; v_r] W_s \quad (2)$$

where $s_{nn'} \in \mathbb{R}$ is the importance score, $v_n, v_{n'} \in \mathbb{R}^M$ are the embedded vectors of nodes n and n' , and $v_r \in \mathbb{R}^D$ is the embedded vector for the direction r associated with node n . $v_n, v_{n'}$ and v_r are all obtained from the embedding layer. $W_s \in \mathbb{R}^{(2M+D) \times 1}$ is the weight matrix of a shared linear transformation applied to every node. Note that we incorporate direction features in the importance score computation so that vehicles passing the same intersection from different directions may result in different importance scores. The incorporation of direction features can capture the dynamic spatial dependencies under different scenarios.

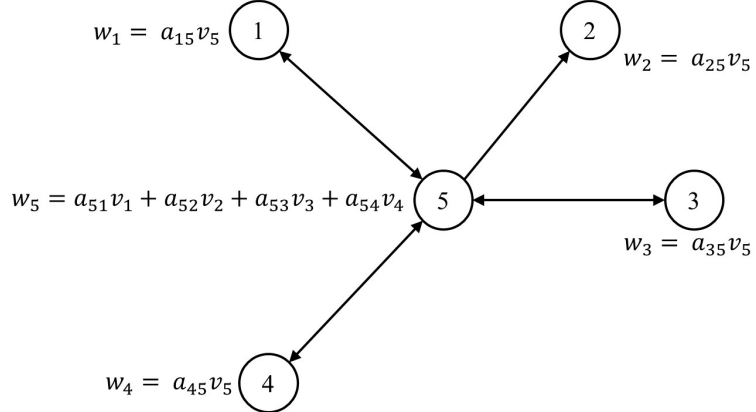


Figure 4: Spatial attention: for each node n in trajectories, a spatial context vector w_n is computed as a weighted sum of the features of its adjacent nodes in the road network.

Step 3: Normalize the importance score using softmax function:

$$a_{nn'} = \frac{\exp(s_{nn'})}{\sum_{n'' \in n.\text{neighbor}} \exp(s_{nn''})} \quad (3)$$

where $a_{nn'} \in \mathbb{R}$ is the attention weight of adjacent node n' to current node n .

Step 4: Compute the context vector w_n as a weighted sum of the features of neighborhood nodes and attention weights:

$$w_n = \sum_{n' \in n.\text{neighbor}} a_{nn'} v_{n'} \quad (4)$$

where $v_{n'} \in \mathbb{R}^M$ is the embedded vector of node n' obtained from the embedding layer.

3.5 LSTM Encoder-decoder with Temporal Attention Mechanisms

Seq2seq models typically have an encoder-decoder structure. The encoder reads and summarizes the input sequence to an internal representation. The decoder then uses the internal representation to generate an output sequence one element at a time. To capture the temporal dependencies within trajectories, we adopt the LSTM encoder-decoder architecture, which is the state-of-the-art architecture for the trajectory prediction problem [7, 8]. In this paper, we represent LSTM as:

$$h_t, c_t = \text{LSTM}(x_t, h_{t-1}, c_{t-1}) \quad (5)$$

where $h_t, c_t \in \mathbb{R}^B$ are cell memory state vector and hidden state vector respectively, B is the dimension of hidden state vector.

3.5.1 Encoder

The input of the encoder is the input node sequence X_N and direction sequence X_R . The encoder consists of S stacked LSTM layers. At each time step, given n_i and r_i , we learn the embedded vectors v_{n_i} and v_{r_i} from the embedding layer, and then the context vector w_{n_i} from the spatial attention layer. The input vector x_i of the recurrent unit is thus defined as the concatenation of the generated representations, i.e., $x_i = [v_{n_i}; v_{r_i}; w_{n_i}]$, where $x_i \in \mathbb{R}^{2M+D}$. Then, the encoder recursively takes x_i as the input vector and hidden state vector h_{i-1} from previous recurrent unit to update vectors h_i, c_i at each time step through Eq. (5). After l_{in} time steps, the encoder summarizes the whole input sequence into the final vectors c_0, h_0 and an output sequence of hidden state vectors $H = \{h_{1-l_{in}}, \dots, h_{-1}, h_0\}$.

3.5.2 Decoder

The input of the decoder is the output node sequence Y_N and direction sequence Y_R . Note that the output elements are offset by one position to make sure the prediction for position i only depends on the previously known outputs. The decoder also consists of S stacked LSTM layers. Similar to the encoder, given n_i and r_i , we learn the embedded vectors v_{n_i} and v_{r_i} from the embedding layer, and then the spatial context vector $w_{n_i} \in \mathbb{R}^B$ from the spatial attention layer. In addition, a temporal context vector u_i is learned from a temporal attention layer that will be introduced later. The input

vector for the decoder is $x'_i = [v_{n_i}; v_{r_i}; w_{n_i}; u_i]$, where $x'_i \in \mathbb{R}^{2M+D+B}$. The decoder uses h_0 and c_0 passed from the encoder as its initial hidden state vector and cell memory state vector. By feeding x'_i, h_{i-1}, c_{i-1} to the recurrent unit recursively using Eq. (5), the output sequence of hidden state vectors $H' = \{h_1, h_2, \dots, h_{l_{out}}\}$ is generated.

3.5.3 Sliding Temporal Attention Layer

Temporal attention mechanisms can capture long-term temporal dependencies by adaptively paying more attention to relevant hidden states in the encoder output sequence H during future sequence generation. It has shown effectiveness in applications such as machine translation [27] and human mobility prediction [32]. Vehicle trajectory prediction is different from previous applications, because the prediction of the next path relies highly on current state. To capture such temporal dependencies in the temporal attention mechanism, we define a sliding temporal context window $[i - l_{in}, i)$ for each time step i , and the sequence H is updated as $\{h_{i-l_{in}}, \dots, h_{-1}, h_0, h_1, h_2, \dots, h_{i-1}\}$. A weighted sum of hidden state vectors in the updated sequence $u_i \in \mathbb{R}^B$ is generated to capture temporal dependencies using:

$$u_i = \sum_{j=i-l_{in}}^{i-1} z_{ij} h_j \quad (6)$$

$$z_{ij} = \frac{\exp(s_{ij})}{\sum_{m=i-l_{in}}^{i-1} \exp(s_{im})} \quad (7)$$

$$s_{ij} = [h_{i-1}; c_{i-1}; h_j] W_t \quad (8)$$

where $W_t \in \mathbb{R}^{(1+2S) \times B}$ is the weight matrix for attention weight computation. Fig. 5 illustrates the mechanism of the sliding temporal attention layer.

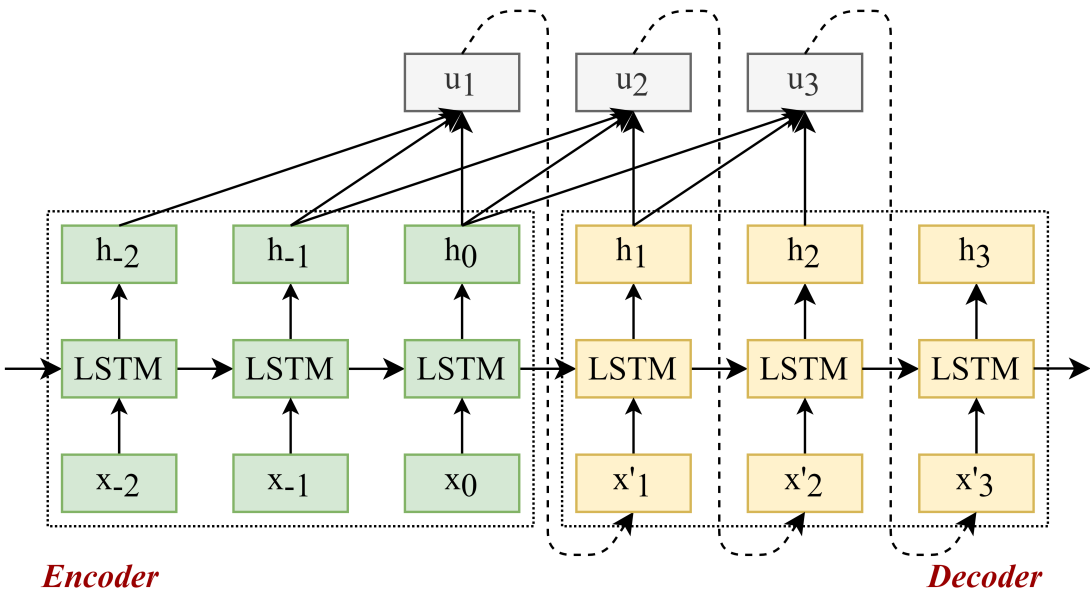


Figure 5: Sliding temporal attention: for each position i in the decoder, a context window $[i - l_{in}, i)$ is used to compute a temporal context vector u_i , which is a weighted sum of the hidden states in the window.

3.6 Output Layer

The output layer predicts the subsequent direction sequence given the decoder output sequence H' from the LSTM encoder-decoder. We also incorporate context features which may also influence drivers' route decisions in the prediction, including time, individual preferences and inclement weather. In our work, the continuous timestamp is divided into $7 \times 24 = 168$ intervals which represents each hour in a week. In addition, we represent weather information as a categorical variable (sunny/cloudy/small rain/rain/heavy rain), and individual information as a unique driver or vehicle identifier representing the inherent routing preferences of each driver. The context features are first mapped to continuous representations using the same embedding method as the embedding layer and then concatenated with the

decoder output sequence H' . Finally, a simple linear layer is adopted to map the concatenated representation to the dimension of directions K and a softmax function is applied to estimate the probability of each direction.

$$Y_{out} = \text{softmax}([H'; V_{time}; V_{weather}; V_{individual}]W_c) \quad (9)$$

where $V_{time} \in \mathbb{R}^{l_{out} \times Q_{time}}$, $V_{weather} \in \mathbb{R}^{l_{out} \times Q_{weather}}$, and $V_{individual} \in \mathbb{R}^{l_{out} \times Q_{individual}}$ are the embedded vectors for time, weather and individual information, and $W_c \in \mathbb{R}^{(B+Q_{time}+Q_{weather}+Q_{individual}) \times K}$ is the parameter matrix for linear transformation.

3.7 Model Setup

3.7.1 Loss function

the prediction of future directions is essentially to classify which direction the vehicle will next visit. Following studies of multi-class classification, we use cross entropy as the loss function to train the model.

$$\text{loss}(\Theta) = - \sum_{i=1}^{l_{out}} \sum_{r=1}^K o_i^r \ln \hat{P}(o_i^r) \quad (10)$$

where Θ denotes the set of parameters in our model, $o_i^r \in \mathbb{R}$ is a dummy variable indicating whether r is the target direction at the i -th position in target trajectory and $\hat{P}(o_i^r)$ is its corresponding probability predicted by the model.

3.7.2 Scheduled Sampling

the input of the decoder during training is the output trajectories with one position offset so that the decoder generates predictions given previously known ground truth observations. In model testing, ground truth observations are replaced by predictions generated by the model itself. Specifically, the most likely direction is selected as the predicted direction and the predicted intersection node is obtained using algorithm 1. To mitigate the discrepancy between the input distributions of training and testing, we incorporate scheduled sampling [35] in the model. During the training process, the model is fed with either the ground truth observation with probability α or the predicted result with probability $1 - \alpha$, and α gradually decreases to 0 as the iteration increases.

4 Experiments

In this section, we evaluate our proposed model by conducting extensive experiments on two real-world vehicle trajectory datasets, and compare it against other state-of-the-art methods.

4.1 Datasets

Shanghai Taxi Trajectory Data (Shanghai Dataset): The dataset is retrieved from one of the major taxi companies in Shanghai which contains the GPS traces of 7579 taxis from 2015-04-15 to 2015-04-21 in Shanghai, China. The average sampling rate is roughly every 10 seconds, and there are over 4 million records in the dataset. Each record consists of the information of taxi ID, date, time, longitude, latitude and occupied flag, which is a binary indicator flagging whether the taxi is occupied. In our experiment, we take trajectories within a bounding box: [30.85, 31.42, 121.08, 121.85]. The road network is obtained from OpenStreetMap using an open-source tool OSMnx [36]. The road network consists of 42,990 intersection nodes and 105,426 road segments as shown in Fig. 6a.

Beijing Taxi Trajectory Data (Beijing Dataset)[37]: This dataset is obtained from the T-Drive project which contains one-week trajectories of 10,357 taxis from 2008-02-02 to 2008-02-08 in Beijing, China. The average sampling rate is 177 seconds and the total number of records is about 15 million. Each record consists of the information of date, time, longitude and latitude. Similarly, we take trajectories within a bounding box: [39.74, 40.05, 116.14, 116.60]. The road network is also obtained from OpenStreetMap, consisting of 30,383 intersection nodes and 69,849 road segments as shown in Fig. 6b.

In addition to taxi GPS data and road network data, we collect weather data from Weather Underground Website. The dataset provides weather condition (e.g., fair, cloudy, rain, storm) every half an hour for Shanghai Data and every 2-3 hours for Beijing Data.

4.2 Data Preprocessing

For Shanghai Dataset, we adopt our proposed data preprocessing approach introduced in a previous paper [38] to extract valid taxi trips from the raw data. After data preprocessing, the possible states of taxis are assigned to the trajectories

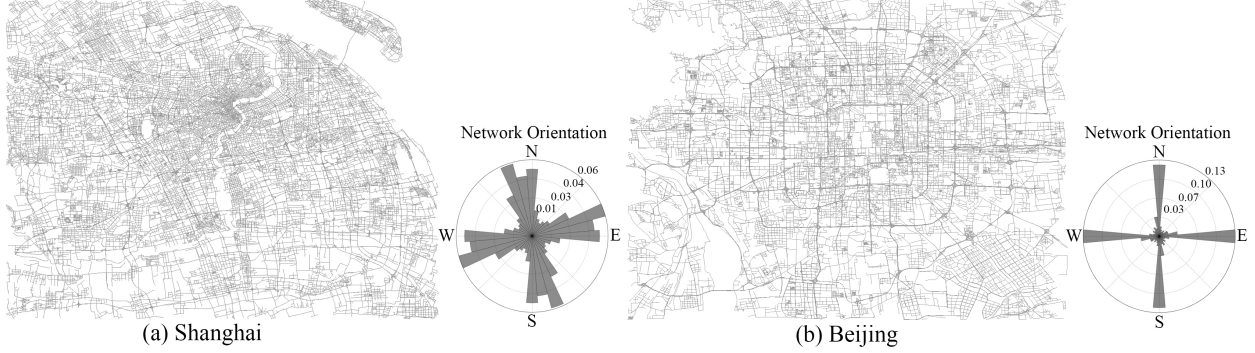


Figure 6: Road networks used in our trajectory prediction experiments

and invalid trips during which taxis are off-shift or taking a short break are filtered. As most vehicles on the road are en route to their destinations, we exclude cruising taxi trips in the following experiments because their routing patterns are quite different. Beijing Dataset does not contain an occupied flag and is generally more sparse, so we cannot segment taxi trajectories based on the occupancy status. Instead, we simply split the trajectory of each driver to multiple sub-trajectories of 50 records with an average time length of 2.5h. To obtain the trajectories as a sequence of road segments, we use an open-source map matching framework called Fast Map Matching [39] which provides an implementation of the ST-Match map mapping approach [18]. The training, validation and test sets are split randomly for both datasets. Table 1 shows the training, validation and test size of both datasets after data preprocessing. To create input and output sequences X and Y , we adopt a segmentation method commonly employed in machine translation [28] and time series analysis [40]. In the first step, we concatenate the input-output trajectories in a single sequence and divide it into batches of size C by trimming off remaining tokens, which allows more efficient batch processing. The second step is to use a sliding window of size Z to reduce the data to input sequences of length l_{in} and output sequences of length l_{out} . For instance, for a training set containing L trajectories with lengths of $\{l_1, l_2, \dots, l_L\}$, the training set will be divided into C sequences of length $l_s = \lfloor \frac{\sum_j^L l_j}{C} \rfloor$. For each sequence T at the i -th prediction step, the input trajectory is $T_{z \times i: z \times i + l_{in}}$ and the output trajectory is $T_{z \times i + l_{in}: z \times i + l_{in} + l_{out}}$.

Table 1: Training, validation and test set description

Dataset	SH	BJ
Total Trajectories (Avg. Length)	520,890 (65)	149,105 (255)
Training Set (Avg. Length)	500,890 (65)	139,105 (255)
Validation Set (Avg. Length)	10,000 (65)	5,000 (259)
Test Set (Avg. Length)	10,000 (65)	5,000 (251)

4.3 Evaluation Metrics

In our experiments, we evaluate the performance of our vehicle trajectory prediction method using the following metrics:

- *Distance Error (DE)*: the average edit distance between predicted and actual trajectories. Edit distance has been commonly used to quantify the similarity between two sequences by counting the minimum number of operations required to transform one sequence to the other. The formula of DE is defined as:

$$DE = \frac{1}{L' l_{out}} \sum_{i=1}^{L'} \text{Edit}(\hat{Y}_i, Y_i) \quad (11)$$

where L' is the number of trajectories in the test set, \hat{Y}_i, Y_i are the i th predicted and true trajectories respectively and $\text{Edit}(\hat{Y}_i, Y_i)$ is the edit distance between the two.

- *Average Match Ratio (AMR)*: the average ratio of the number of correctly predicted road segments to the length of predicted trajectories. The formula of MR is defined as:

$$AMR = \frac{1}{L' l_{out}} \sum_{i=1}^{L'} \sum_{j=1}^{l_{out}} \text{Match}(\hat{e}_j^i, e_j^i) \quad (12)$$

where \hat{e}_j^i, e_j^i are the predicted and true road segment in the j -th position of the i -th trajectory. $Match(\hat{e}_j^i, e_j^i) = 1$ if they are the same and 0 otherwise.

- *Match Ratio(k) ($MR(k)$)*: the ratio of the number of trajectories with at least k road segments correctly predicted to the number of total trajectories L' , where $k = 1, \dots, l_{out}$. For example, $MR(l_{out})$ refers to the likelihood of correctly predicting every road segment in a trajectory. The formula of $MR(k)$ is defined as:

$$MR(k) = \frac{1}{L'} \sum_{i=1}^{L'} Match_k(\hat{Y}_i, Y_i) \quad (13)$$

where $Match_k(\hat{Y}_i, Y_i) = 1$ if $\sum_{j=1}^{l_{out}} Match(\hat{e}_j^i, e_j^i) \geq k$ and 0 otherwise. By definition, $Match_k(\hat{Y}_i, Y_i)$ decreases with k .

4.4 Settings

All experiments are conducted on a NVIDIA 1080 Ti GPU. We use the stochastic gradient descent optimizer with the batch size of 20, the sliding window size of 5 and the dropout rate of 0.1. The initial learning rate is set to 0.5, and it decays at a rate of 0.8 every epoch. Through intensive empirical optimization, we determine the hyperparameters of our proposed model as:

- The number of directions $K = 8$
- The embedding dimensions of node and direction sequences $M = D = 256$
- The hidden dimension of the LSTM encoder-decoder network $B = 512$
- The depth of LSTM stack $S = 2$
- The embedding dimensions of context features $Q_{time} = Q_{weather} = Q_{individual} = 32$
- The length of an input trajectory $l_{in} = 10$
- The length of an output trajectory $l_{out} = 5$

4.5 Baseline Models

As introduced in Section 2, existing vehicle trajectory prediction mostly adopted probabilistic graphical models and there is no existing deep learning-based method for vehicle trajectory prediction in a city-scale road network. Therefore, we implement several seq2seq models adapted from the literature, in addition to a basic markov chain model, for benchmarking. The baseline models include:

- *Markov Chain (MC)*. We use a first-order Markov Chain, or MC(1), as a benchmark method, which can be extended to predict a sequence of road segments iteratively by conditioning on the previous known or predicted road segments.
- *LSTM Encoder-decoder (LSTM)*. A LSTM encoder-decoder architecture was adopted by [7] for vehicle trajectory prediction on an occupancy grid map. For comparison, a similar model is implemented for vehicle trajectory prediction in road networks. Specifically, the encoder takes an input intersection node sequence and the decoder generates a future node sequence.
- *Temporal Attention-based LSTM Encoder-decoder (T-LSTM)*. Capobianco et al. [40] proposed a vessel trajectory prediction model based on LSTM encoder-decoder and applied an attention mechanism to aggregate the encoder outputs. We implement a similar model which inputs the latest intersection node sequence and generates a future node sequence for comparison.
- *Transformer (TA)*. First proposed by [28] for machine translation, Transformer has not been used for vehicle trajectory prediction yet. In this research, we design and develop a Transformer network for vehicle trajectory prediction by regarding each trajectory as a sentence and each intersection node a word.

4.6 Prediction Performance

The results are shown in Table 2. We can observe that for both datasets, the proposed model achieves superior performance than baseline models. In comparison of the state-of-the-art methods, our model shows 9.6% and 4.5% reduction in DE for Shanghai dataset and Beijing dataset respectively. This is potentially because existing deep learning methods only capture temporal dependencies while our proposed model also captures spatial dependencies in the road

network with the spatial attention layer. Our model also takes advantage of direction-based trajectory representation that reduces the output dimension and thus simplifies the prediction task. In addition, we adopt a different temporal attention mechanism with sliding temporal context window to capture both long-term and short-term temporal dependencies. As shown in Fig. 7, for both Shanghai and Beijing, our model outperforms the baseline methods regarding $MR(k)$, and the gap increases with k . This is likely due to error propagation, since the quality of long-range predictions relies on short-range prediction accuracies. Fig. 8 shows a few example trajectories from the Shanghai dataset and corresponding predictions based on D-LSTM, demonstrating the effectiveness of our proposed model in predicting vehicle trajectories under diverse road network scenarios.

Table 2: The performance comparison of different models on Shanghai and Beijing Datasets

Model	Shanghai			Beijing		
	DE (%)	AMR (%)	Time (h/ep)	DE (%)	AMR (%)	Time (h/ep)
MC	47.0	52.8	-	34.1	65.8	-
LSTM	37.7	62.0	2.15	31.7	68.1	2.85
T-LSTM	37.5	62.2	3.63	31.6	68.3	4.82
TA	38.0	61.7	1.88	31.5	68.4	2.53
D-LSTM	33.9	65.8	2.75	30.1	69.7	3.61

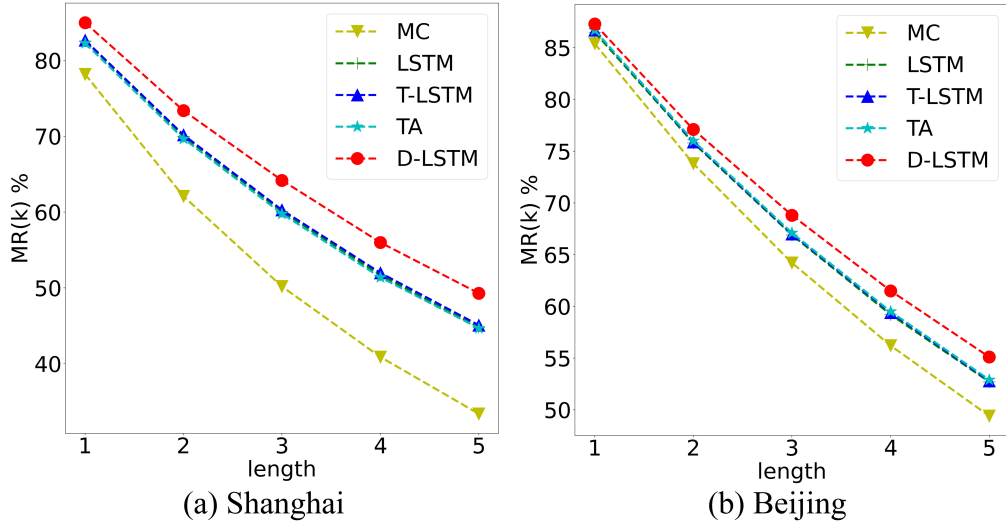


Figure 7: The $MR(k)$ of different trajectory lengths

Comparing the two datasets, we find that the overall prediction performance in Beijing is consistently better than in Shanghai. The AMR of Beijing dataset is 24.6% higher than Shanghai data using MC, and 6.4% - 10.9% higher than Shanghai using seq2seq models. This is potentially because the road network in Beijing is more regularly structured than in Shanghai. As shown in Fig. 6, Beijing has an obvious grid system organizing city circulation, while Shanghai’s road network has more diverse orientations. This may also explain why D-LSTM shows higher improvement from baseline methods in the Shanghai data. In complex road networks, D-LSTM can significantly improve prediction performance as our proposed direction-based representation can help simplify the road network and the spatial attention mechanism can capture the network structure more efficiently.

Among baseline models, T-LSTM, LSTM and TA all outperform MC by a notable margin for both datasets, indicating the effectiveness of seq2seq models in vehicle trajectory prediction. Compared with MC, LSTM can reduce DE by 19.8% in the shanghai data and 7.0% in the Beijing data. This indicates that seq2seq models are more effective in complex road networks, which is reasonable as deep learning models are better at capturing stochastic relationships in complex environments. The performance difference between LSTM, T-LSTM and TA is not obvious. T-LSTM performs slightly better than LSTM, followed by TA for the Shanghai data, while in Beijing TA slightly outperforms T-LSTM followed by LSTM. This suggests that neither T-LSTM nor TA is able to show consistent improvement in vehicle trajectory prediction across different road networks. While T-LSTM and TA are capable of handling long-term temporal dependencies, the problem of vehicle trajectory prediction seems to mainly rely on short-term dependencies (e.g., the two previous road segments). This can be further confirmed by Table 3, in which we compare the prediction

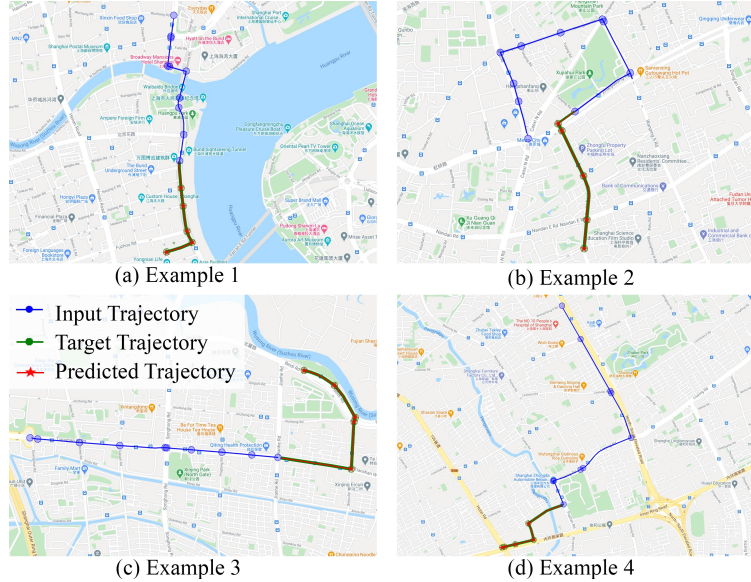


Figure 8: Prediction results in diverse road networks on the Shanghai validation set with D-LSTM

performance of our proposed model with different lengths of input trajectories. It is found that, the AMR can already achieve 62.8% when $l_{in} = 2$, compared to 65.8% when $l_{in} = 10$. This shows that most predictive information can already be captured by the previous two road segments. Table 3 also shows that the prediction performance gradually improves as l_{in} increases. This indicates that while long-term temporal dependency does not contribute much, it still helps with the prediction performance to some extent.

Table 3: The performance comparison of different input trajectory lengths on Shanghai Dataset using D-LSTM

Length	DE (%)	AMR (%)	Shanghai				
			1	2	3	4	5
2	36.9	62.8	83.4	70.8	60.8	52.4	45.9
4	36.3	63.4	83.9	71.5	61.9	53.3	47.1
6	35.3	64.4	84.4	72.2	62.7	54.3	47.9
8	35.0	64.7	84.6	72.4	63.0	54.7	48.2
10	33.9	65.8	85.0	73.4	64.2	56.0	49.3

In comparison of the run time of different models, we can find that TA has the lowest time cost, which is quite reasonable as it skips RNNs and enables better parallelization. LSTM has the second lowest run time, as it has no attention mechanisms and is thus faster than T-LSTM and D-LSTM. While T-LSTM applies only temporal attention and D-LSTM considers both temporal and spatial attentions, the time cost of D-LSTM is significantly lower than T-LSTM, which can be explained by the dimension reduction of the output sequences through the direction-based representation.

4.7 Ablation Study

In this section, we conduct extensive ablation studies to quantify the contributions of different components in the proposed model. Since the Shanghai data is more challenging to predict than the Beijing data, we will focus on the Shanghai case here. We denote the base model as D-LSTM and drop different components to construct variants, which will be tested and compared against the full model. The components are listed as:

- *Direction-based Trajectory Representation (D-TR)*. This denotes the trajectory representation module that transforms a vehicle trajectory to a node sequence and a direction sequence. D-TR allows us to simply predict the direction sequence, which greatly simplifies the prediction problem. With D-TR ablated, both the input and output trajectories are a sequence of intersection nodes.
- *Dynamic Spatial Attention (DSA)*. This denotes the spatial attention module used to capture spatial dependencies in road networks. Two models are developed to illustrate the effectiveness of dynamic spatial attention:

one replaces DSA with fixed spatial attention module (FSA) in which direction is not incorporated in the computation of spatial attention, and the other drops the spatial attention module.

- *Sliding Temporal Attention (STA)*. This denotes the temporal attention module used to capture temporal dependencies in trajectories. Two models are developed to illustrate the effectiveness of sliding temporal attention: one adopts fixed temporal attention module (FTA) in which the temporal attention module aggregates the encoder outputs using attention mechanism, and the other drops the temporal attention module.

Table 4: The performance comparison of different components of D-LSTM on Shanghai Dataset

Model	DE (%)	AMR (%)	Shanghai					Time (h/ep)
			1	2	3	4	5	
D-LSTM	33.9	65.8	85.0	73.4	64.2	56.0	49.3	2.75
-D-TR	37.3	62.5	83.4	70.6	60.6	52.0	45.1	4.51
FSA	34.2	65.5	84.8	73.3	64.1	55.8	49.0	2.67
-DSA	34.6	65.1	84.7	72.8	63.5	55.2	48.5	2.32
FTA	34.1	65.6	85.1	73.3	64.1	55.8	48.9	2.71
-DTA	34.3	65.4	84.9	73.1	63.8	55.5	48.7	2.04
-DSA-DTA	35.2	64.5	84.6	72.4	62.9	54.5	47.6	1.68

Table 4 shows the results of the ablation study. We find that the direction-based trajectory representation is crucial for improving both prediction performance and modeling efficiency. Compared with the model without D-TR, the direction-based trajectory representation provides a 9.1% reduction in DE and 39.1% reduction in run time. Compared with the baseline LSTM, the model without DSA or DTA can still reduce DE by 6.6% and improves modeling efficiency by 41.1%, further validating the effectiveness of our direction-based trajectory representation approach.

The attention mechanisms are also shown to improve the model performance, with 3.8% reduction in DE. Compared with the model with no spatial attention at all, fixed spatial attention can lead to a reduction of around 1.2% in DE, and the integration of directions in spatial attention (or dynamic spatial attention) can further improve the prediction performance slightly. In dynamic spatial attention, the direction information is used to capture the different spatial dependencies for vehicles passing the same intersection from different directions. In addition, compared with the model with no temporal attention considered, our proposed sliding temporal attention results in a reduction of around 1.2% in DE, superior to the fixed temporal attention with a 0.6% reduction. This confirms our assumption that the vehicle trajectory prediction problem relies more on short-term temporal dependencies while long-term temporal dependencies only contribute slightly.

4.8 Interpretability Study

To further understand how spatiotemporal dependencies are captured in the D-LSTM model, we visualize the attention weights of spatial attention and temporal attention modules.

Fig. 9a shows the attention weights in spatial attention module for the first two example trajectories displayed in Fig. 8. Recall that the attention weights represent the relative importance of adjacent nodes to a node in a trajectory. Arcs in Fig. 9a denote the attention weights. Red colors indicate greater weights while blue colors indicate lower weights. It is found that, although each node has multiple adjacent nodes, it usually pays specifically high attention to only one adjacent node. To uncover the mobility patterns underlying in spatial attention weights, we further visualize the transition probabilities between intersection nodes, i.e., the observed probabilities of vehicles moving from a node to another, as shown in Fig. 9b. Most of the red-highlighted adjacent nodes in Fig. 9a are also highlighted in Fig. 9b, indicating that the spatial attention mechanism can to some extent capture the transition probabilities between intersections. However, differences do exist in these two figures, indicating that spatial dependencies of intersections in a road network may vary with driving directions and context features.

Fig. 10 shows the attention weights in temporal attention module for the same example trajectories displayed in Fig. 9. Each heatmap has $l_{out} = 5$ rows and $l_{in} = 10$ columns, and each element in the heatmap shows how each road segment (1-10) in the temporal context window influences each predicted road segment (1-5). As shown in Fig. 10, the temporal attention weight is more evenly distributed than the spatial attention. An interesting observation is that the attention weights on the same diagonal are almost the same. Recall that we adopt a sliding context window for temporal attention computation. This indicates that the weighted influence of the same road segment in the input trajectory to different road segments in the output trajectory is mostly the same. We can also find that, in the input trajectory, road segments that are closer to the output trajectory generally have higher attention weights, validating our assumption that trajectory prediction mainly relies on short-term dependency.

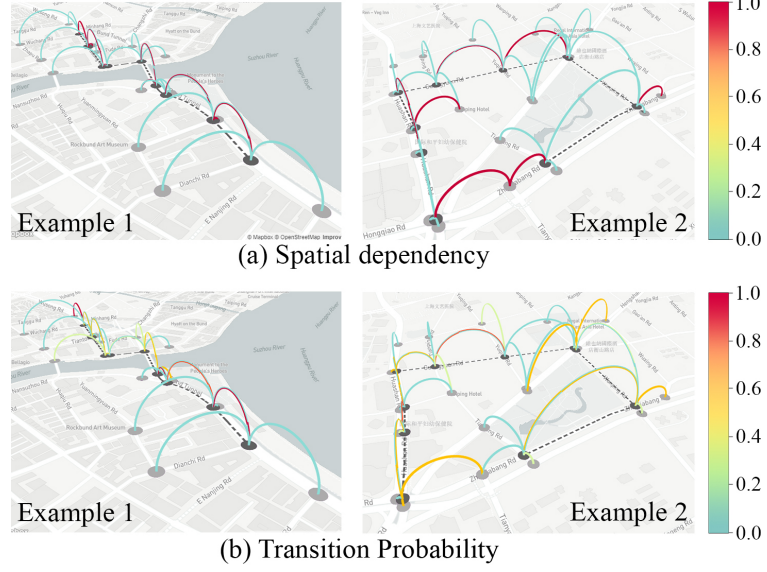


Figure 9: The spatial attention of the input trajectories of the first two examples displayed in Fig. 8. (Dark grey dashed lines represent the input trajectories, dark grey points represent the intersection nodes in trajectories, and light grey points represent the adjacent nodes.)

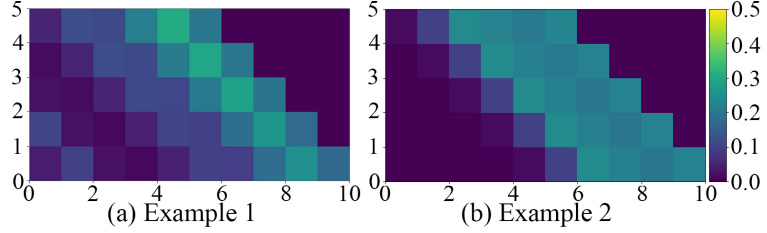


Figure 10: The temporal attention weight matrix of the first two examples displayed in Fig. 8 (the x axis represents the position in the sliding temporal window and the y axis represents the output length)

5 Conclusion

Trajectory prediction of vehicles at the city scale is of great importance to various location-based applications such as vehicle navigation, traffic management, and location-based recommendations. In this paper, we propose a novel direction-based seq2seq model with spatiotemporal attention mechanisms, named D-LSTM, for vehicle trajectory prediction in city-scale road networks. Unlike existing methods that represent trajectories as sequences of grid cells, road segments or driver intentions, we propose a direction-based trajectory representation approach which represents each trajectory as a sequence of intersections and associated movement directions. This new representation greatly simplifies the trajectory prediction problem and improves both the prediction accuracy and modeling efficiency. To capture the dynamic spatial dependencies in road networks, a spatial attention module is introduced, in which the road network is treated as a graph and adjacent intersections (nodes) pass messages to each other. Finally, a LSTM encoder-decoder network with a sliding temporal attention mechanism is adopted to capture both long-term and short-term temporal dependencies. Experiments on two real-world taxi trajectory datasets show that D-LSTM can achieve superior prediction performance than state-of-the-art algorithms.

There are several directions for future research. First, some specific physical attributes of road segments are not considered in our model due to lack of data, and road attributes such as type of road, speed limit, real-time traffic may also affect vehicle driving behaviors. Second, our proposed trajectory representation approach is developed for 2D road networks while future studies can extend it to 3D network structure, such as 3D pedestrian networks with overpasses and underground tunnels. This is particularly useful for cities like Hong Kong with 3D transportation networks. Third, existing studies mostly focus on trajectory prediction for vehicles en route to a destination. However, sometimes vehicles do not have a clear or fixed destination, e.g., cars cruising for parking space or taxis cruising for passengers. The routing patterns of cruising vehicles are quite different, as their goal is no longer to find the fastest path to some

places. Trajectory prediction of cruising vehicles can provide trajectory-level cruising strategies, improve the efficiency of urban traffic systems and reduce the number of vehicles on the road.

Acknowledgments

The computations were performed using research computing facilities offered by Information Technology Services, the University of Hong Kong.

References

- [1] Brian D Ziebart, Andrew L Maas, Anind K Dey, and J Andrew Bagnell. Navigate like a cabbie: Probabilistic reasoning from observed context-aware behavior. In *Proceedings of the 10th international conference on Ubiquitous computing*, pages 322–331, 2008.
- [2] Li Li, Rui Jiang, Zhengbing He, Xiqun Michael Chen, and Xuesong Zhou. Trajectory data-based traffic flow studies: A revisit. *Transportation Research Part C: Emerging Technologies*, 114:225–240, 2020.
- [3] Xiangjie Kong, Feng Xia, Jinzhong Wang, Azizur Rahim, and Sajal K Das. Time-location-relationship combined service recommendation based on taxi trajectory data. *IEEE Transactions on Industrial Informatics*, 13(3):1202–1212, 2017.
- [4] Punit Rathore, Dheeraj Kumar, Sutharshan Rajasegarar, Marimuthu Palaniswami, and James C Bezdek. A scalable framework for trajectory prediction. *arXiv preprint arXiv:1806.03582*, 2018.
- [5] Reid Simmons, Brett Browning, Yilu Zhang, and Varsha Sadekar. Learning to predict driver route and destination intent. In *2006 IEEE Intelligent Transportation Systems Conference*, pages 127–132. IEEE, 2006.
- [6] Shaojie Qiao, Dayong Shen, Xiaoteng Wang, Nan Han, and William Zhu. A self-adaptive parameter selection trajectory prediction approach via hidden markov models. *IEEE Transactions on Intelligent Transportation Systems*, 16(1):284–296, 2014.
- [7] Seong Hyeon Park, ByeongDo Kim, Chang Mook Kang, Chung Choo Chung, and Jun Won Choi. Sequence-to-sequence prediction of vehicle trajectory via lstm encoder-decoder architecture. In *2018 IEEE Intelligent Vehicles Symposium (IV)*, pages 1672–1678. IEEE, 2018.
- [8] Hang Zhao, Jiyang Gao, Tian Lan, Chen Sun, Benjamin Sapp, Balakrishnan Varadarajan, Yue Shen, Yi Shen, Yuning Chai, Cordelia Schmid, et al. Tnt: Target-driven trajectory prediction. *arXiv preprint arXiv:2008.08294*, 2020.
- [9] Yu Wang, Shengjie Zhao, Rongqing Zhang, Xiang Cheng, and Liuqing Yang. Multi-vehicle collaborative learning for trajectory prediction with spatio-temporal tensor fusion. *IEEE Transactions on Intelligent Transportation Systems*, 2020.
- [10] Sajjad Mozaffari, Omar Y Al-Jarrah, Mehrdad Dianati, Paul Jennings, and Alexandros Mouzakitis. Deep learning-based vehicle behavior prediction for autonomous driving applications: A review. *IEEE Transactions on Intelligent Transportation Systems*, 2020.
- [11] Alex Zyner, Stewart Worrall, and Eduardo Nebot. A recurrent neural network solution for predicting driver intention at unsignalized intersections. *IEEE Robotics and Automation Letters*, 3(3):1759–1764, 2018.
- [12] Wenchao Ding, Jing Chen, and Shaojie Shen. Predicting vehicle behaviors over an extended horizon using behavior interaction network. In *2019 International Conference on Robotics and Automation (ICRA)*, pages 8634–8640. IEEE, 2019.
- [13] Shaojie Qiao, Nan Han, Junfeng Wang, Rong-Hua Li, Louis Alberto Gutierrez, and Xindong Wu. Predicting long-term trajectories of connected vehicles via the prefix-projection technique. *IEEE Transactions on Intelligent Transportation Systems*, 19(7):2305–2315, 2017.
- [14] Jingbo Zhou, Anthony KH Tung, Wei Wu, and Wee Siong Ng. A “semi-lazy” approach to probabilistic path prediction in dynamic environments. In *Proceedings of the 19th ACM SIGKDD international conference on Knowledge discovery and data mining*, pages 748–756, 2013.
- [15] Philip Pecher, Michael Hunter, and Richard Fujimoto. Data-driven vehicle trajectory prediction. In *Proceedings of the 2016 ACM SIGSIM Conference on Principles of Advanced Discrete Simulation*, pages 13–22, 2016.
- [16] Patrick Ebel, Ibrahim Emre Göl, Christoph Lingenfelder, and Andreas Vogelsang. Destination prediction based on partial trajectory data. In *2020 IEEE Intelligent Vehicles Symposium (IV)*, pages 1149–1155. IEEE, 2020.

[17] Jianming Lv, Qing Li, Qinghui Sun, and Xintong Wang. T-conv: A convolutional neural network for multi-scale taxi trajectory prediction. In *2018 IEEE international conference on big data and smart computing (bigcomp)*, pages 82–89. IEEE, 2018.

[18] Yin Lou, Chengyang Zhang, Yu Zheng, Xing Xie, Wei Wang, and Yan Huang. Map-matching for low-sampling-rate gps trajectories. In *Proceedings of the 17th ACM SIGSPATIAL international conference on advances in geographic information systems*, pages 352–361, 2009.

[19] Xiong Liu and Hassan A Karimi. Location awareness through trajectory prediction. *Computers, Environment and Urban Systems*, 30(6):741–756, 2006.

[20] Jinjun Tang, Jian Liang, Shen Zhang, Helai Huang, and Fang Liu. Inferring driving trajectories based on probabilistic model from large scale taxi gps data. *Physica A: Statistical Mechanics and its Applications*, 506:566–577, 2018.

[21] Andy Yuan Xue, Jianzhong Qi, Xing Xie, Rui Zhang, Jin Huang, and Yuan Li. Solving the data sparsity problem in destination prediction. *The VLDB Journal*, 24(2):219–243, 2015.

[22] Derek J Phillips, Tim A Wheeler, and Mykel J Kochenderfer. Generalizable intention prediction of human drivers at intersections. In *2017 IEEE intelligent vehicles symposium (IV)*, pages 1665–1670. IEEE, 2017.

[23] Akinori Asahara, Kishiko Maruyama, Akiko Sato, and Kouichi Seto. Pedestrian-movement prediction based on mixed markov-chain model. In *Proceedings of the 19th ACM SIGSPATIAL international conference on advances in geographic information systems*, pages 25–33, 2011.

[24] Sébastien Gambs, Marc-Olivier Killijian, and Miguel Núñez del Prado Cortez. Next place prediction using mobility markov chains. In *Proceedings of the first workshop on measurement, privacy, and mobility*, pages 1–6, 2012.

[25] Zhan Zhao, Haris N. Koutsopoulos, and Jinhua Zhao. Individual mobility prediction using transit smart card data. *Transportation Research Part C: Emerging Technologies*, 89:19–34, April 2018.

[26] Baichuan Mo, Zhan Zhao, Haris N. Koutsopoulos, and Jinhua Zhao. Individual mobility prediction: An interpretable activity-based hidden markov approach. *arXiv preprint arXiv:2101.03996*, 2021.

[27] Dzmitry Bahdanau, Kyunghyun Cho, and Yoshua Bengio. Neural machine translation by jointly learning to align and translate. *arXiv preprint arXiv:1409.0473*, 2014.

[28] Ashish Vaswani, Noam Shazeer, Niki Parmar, Jakob Uszkoreit, Llion Jones, Aidan N Gomez, Łukasz Kaiser, and Illia Polosukhin. Attention is all you need. *arXiv preprint arXiv:1706.03762*, 2017.

[29] Mike Schuster and Kuldip K Paliwal. Bidirectional recurrent neural networks. *IEEE transactions on Signal Processing*, 45(11):2673–2681, 1997.

[30] Sepp Hochreiter and Jürgen Schmidhuber. Long short-term memory. *Neural computation*, 9(8):1735–1780, 1997.

[31] Junyoung Chung, Caglar Gulcehre, KyungHyun Cho, and Yoshua Bengio. Empirical evaluation of gated recurrent neural networks on sequence modeling. *arXiv preprint arXiv:1412.3555*, 2014.

[32] Fa Li, Zhipeng Gui, Zhaoyu Zhang, Dehua Peng, Siyu Tian, Kunxiaoja Yuan, Yunzeng Sun, Huayi Wu, Jianya Gong, and Yichen Lei. A hierarchical temporal attention-based lstm encoder-decoder model for individual mobility prediction. *Neurocomputing*, 403:153–166, 2020.

[33] Yadong Li, Bailong Liu, Lei Zhang, Susong Yang, Changxing Shao, and Dan Son. Fast trajectory prediction method with attention enhanced sru. *IEEE Access*, 8:206614–206621, 2020.

[34] Petar Veličković, Guillem Cucurull, Arantxa Casanova, Adriana Romero, Pietro Lio, and Yoshua Bengio. Graph attention networks. *arXiv preprint arXiv:1710.10903*, 2017.

[35] Samy Bengio, Oriol Vinyals, Navdeep Jaitly, and Noam Shazeer. Scheduled sampling for sequence prediction with recurrent neural networks. *arXiv preprint arXiv:1506.03099*, 2015.

[36] Geoff Boeing. Osmnx: New methods for acquiring, constructing, analyzing, and visualizing complex street networks. *Computers, Environment and Urban Systems*, 65:126–139, 2017.

[37] Jing Yuan, Yu Zheng, Chengyang Zhang, Wenlei Xie, Xing Xie, Guangzhong Sun, and Yan Huang. T-drive: driving directions based on taxi trajectories. In *Proceedings of the 18th SIGSPATIAL International conference on advances in geographic information systems*, pages 99–108, 2010.

[38] Yuebing Liang and Zhan Zhao. Mining factors affecting taxi cruising time using gps traces. *Computers, Environment and Urban Systems*, under review.

[39] Can Yang and Gyozo Gidofalvi. Fast map matching, an algorithm integrating hidden markov model with precomputation. *International Journal of Geographical Information Science*, 32(3):547–570, 2018.

[40] Samuele Capobianco, Leonardo M Millefiori, Nicola Forti, Paolo Braca, and Peter Willett. Deep learning methods for vessel trajectory prediction based on recurrent neural networks. *arXiv preprint arXiv:2101.02486*, 2021.